The Abdus Salam
International Centre for Theoretical Physics

United Nations
Educational, Scientific and
Cultural Organization

IAEA
International Atomic Energy Agency

**1867-54**

# College of Soil Physics

***22 October - 9 November, 2007***

## SOIL WATER RETENTION CURVE, INTERPRETATION

Miroslav Kutilek
*Nad Patankou 34, 160 00 Prague 6*
*Czech Republic*

**ICTP TRIESTE**
**COLLEGE ON SOIL PHYSICS 2007**

---

# SOIL WATER RETENTION CURVE, INTERPRETATION

LECTURE NOTES

M. KUTÍLEK, D.R. NIELSEN, K. REICHARDT

(Partly excerpt from: M. Kutílek and D.R. Nielsen, 1994, Soil Hydrology, Catena Verlag, pp. 102-120)

## 1. Soil water retention curve (SWRC)

We have demonstrated that a particular soil water potential $\phi_w$ is related to the soil water content $\theta$. The potential $\phi_w$ is usually expressed as pressure head $h$ [cm] for the convenience of computation and measuring technique. The functional relationship $h(\theta)$ is typical for the given soil having its particular status of consolidation, geometrical arrangement of particles and aggregation and other chemical and biological features. The function $h(\theta)$ when plotted is called a soil water retention curve SWRC, see Fig. 1. In the literature, the terms capillary pressure curve (Dullien, 1979) or soil moisture characteristic curve (Childs, 1969, and Hillel, 1971) has also been used. Because $h$ extends over three to four orders of magnitude for fluctuations of $\theta$ commonly occurring in the field, $h$ is frequently plotted with a logarithmic scale, see Fig. 1.

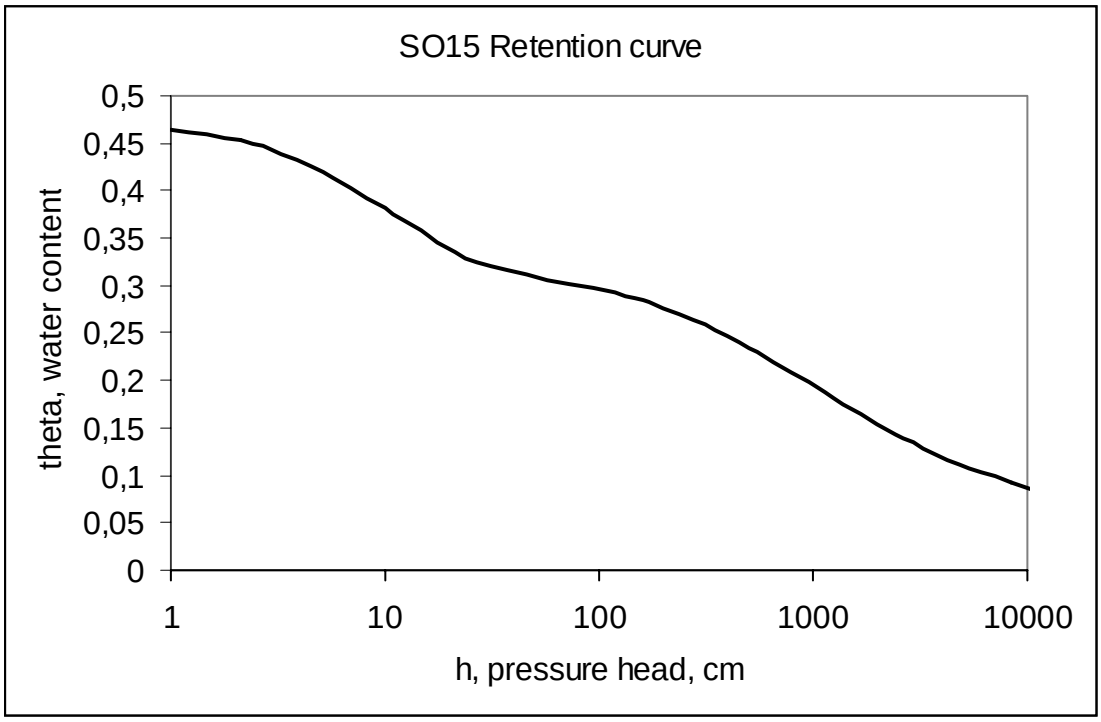


Fig.1. Soil water retention curve

Most often, it is tacitly assumed that $h(\theta)$ is determined at a constant temperature because properties and behavior of the soil water system are temperature dependent, e.g. the surface tension of water. However, in practical studies, the temperature dependence of $h(\theta)$ has been neglected until now without fully demonstrating the range of errors owing to such negligence. We shall say more about it at the end of this chapter.

Similar to the hysteresis of adsorption-desorption isotherms, the soil water retention curve manifests hysteresis. That is, $\theta$ in the drying (or drainage) branch of $h(\theta)$ is larger than $\theta$ in the wetting branch for the same value of $h$.

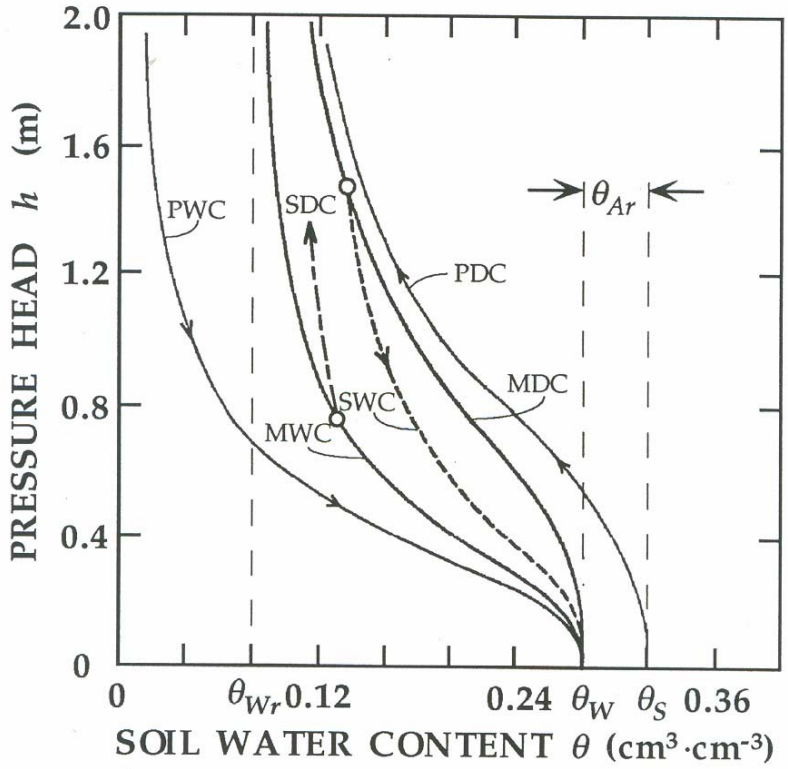


Fig. 2. Hysteresis of the SWRC for a coarse textured soil. PDC is the primary drainage curve, PWC the primary wetting curve, MDC the main drainage curve, MWC the maind wetting curve, SWC a scanning wetting curve and SDC a scanning drainage curve.

In Fig. 2 hysteresis loops of the SWRC are schematically demonstrated. The soil was assumed to be initially fully saturated with water, completely without an air phase, with a saturated water content $\theta_S$ equal to the porosity $P$. Subsequently, the soil was gradually drained and dried, respectively at each $h_j$, the equilibrium $\theta_j$ was determined at sufficient values of $j$ to ascertain the primary drying curve PDC continuously to a soil water content equal to zero. Next, the soil was gradually wetted along several values of $\theta_j$ until the primary wetting curve PWC was measured and at $h = 0$, $\theta = \theta_W$. The wetting curve does not converge to $\theta_S$, and hence, $\theta_W \neq \theta_S$. The volumetric domain $\theta_{Ar} = (\theta_S - \theta_W)$ is filled by an incoherently distributed air phase. This condition is sometimes called entrapped air which we can approximately demonstrate as mutually unconnected micro bubbles of air. Having no chance to escape as a continuous flux, these incoherently distributed micro bubbles of air can only

disappear either by a long lasting process of dissolution and diffusion in soil water, or by a drastic reduction of the pressure of the external atmosphere. When we start now with drainage having $\theta = \theta_W$ at $h = 0$, we obtain a main drainage curve MDC which is not identical to the PDC. If instead of drying the soil to a defined value of $p/p_o < 0.98$ using a controlled humidity chamber, we use a pressure plate apparatus, the MDC will asymptotically approach the "real" residual water content $\theta_{Wr}$ which characterizes the boundary between the coherent and incoherent water phase distributions. Luckner et al. (1989) found the approximate relationship $\theta_{Wr} \approx 2\theta_{Ar}$. The wetting curve which starts at $\theta_{Wr}$ is the main wetting curve MWC, and it is not identical with the PWC. At $h = 0$, the MWC reaches again $\theta_W$. Thus, we obtain a closed hysteretic loop of main curves with an exclusion of the incoherent distribution of air close to $\theta = \theta_S$ and the incoherent distribution of water close to $\theta = 0$ (Luckner et al., 1989). These two incoherent domains of isolated air or water, respectively, are transported by different mechanisms than those for the bulk flux of either of the coherent phases. When drainage on the MDC is interrupted at point $D_1$ by the soil gradually wetting, the scanning wetting curve SWC is "above" the main wetting curve and the values of $\theta$ corresponding to a given h are larger than those on the main wetting curve MWC but smaller than those on the main drainage curve MDC. Similarly, when the wetting along the main wetting curve MWC is interrupted by the soil draining before reaching $\theta_W$, the scanning drainage curve is "below" the MDC. When the hysteretic loop is gradually shortened as in Fig. 2, the scanning curves never intersect each other. Hysteresis is attributed to the action of several factors – the enclosed air in "blind pores", the ink-bottle effect of the influence of the rosary shaped pores where the radius of the meniscus depends upon the direction of reaching a given level and, moreover, the difference in wetting angle occurring for an advancing versus receding liquid front over the solid surface. In our description of hysteresis we could have proceeded vice versa, i.e. we could have started with a completely dry soil at $\theta = 0$.

A treatise on the role of individual factors controlling hysteresis is rather speculative. The theory of independent domains was first applied (Poulovassilis, 1962) and further on, the theory of dependent domains was discussed (Mualem and Miller, 1979, and Mualem, 1984). Both approaches were based upon the theories of Everett (1954, 1967). The independent domain theory assumes that all pore domains are free to drain independently. In reality, only those pores which have free access to the outside air can drain. This access is dependent upon the state of the surrounding pores – be they water or air filled. To account for this dependence, a domain dependence factor $P_d < 1$ is applied and its relationship to $\theta$ is searched. If $P_d = 1$, the dependent domain model is, in this case, equal to the independent domain model. For the wetting process, the blockage to the entering water is usually assumed to be of negligible importance and the independent domain theory is applied. Direct measurement (CT and NMR) and evaluation of soil porous systems in appropriate models can offer parameters needed for conceptual description of hysteresis.

Generally, hysteresis decreases the rate of change in $\theta$ when wetting is interrupted and replaced by drainage, and vice versa.

## 2. Analysis of Soil Water Retention Curves

Some characteristic values are significant for each SWRC, see Fig. 2. After subjecting a soil for a long period with a pressure head $h = 0$, complete water saturation $\theta_S$ is eventually reached when $\theta_S = P$ the porosity. When the soil is quickly wetted, as is usually the case, 3 to 8% of the soil is occupied by entrapped air. This smallest maximum extreme of $\theta$ is denoted in Fig. 2 as $\theta_W$ with $\theta_W = P(1 - n)$ where $n = 0.05$ to 0.15 even though $h = 0$. On the MDC the

air entry value $h_A$ is sometimes found at the minimum value of $h$ when $d\theta/dh$ remains equal to zero. When the same criterion is applied to the main wetting branch, the water entry value $h_W$ is also similarly defined. However, in some soils, $h_A = h_W = 0$, or more frequently, $h_W = 0$. The air entry value $h_A$ is well defined and well measurable in coarse textured soils and in modeling graded sands in the laboratory. In medium and fine textured field soils the estimation of $h_A$ is inaccurate and some authors pose the question on the existence of $h_A$ in the majority of topsoils (Nielsen et al., 1986). However, in subsoils and in deep layers of sediments, the saturated "capillary fringe" above the zero pressure ground water level is traditionally accepted, thus indicating the existence of both $h_A$ and $h_W$. If macropores as fissures and cavities produced by the edaphon exist in a soil, the value of $\theta$ changes abruptly from $\theta_S$ to $\theta_{SM}$ when $h$ is decreased by an infinitesimally small increment $dh$ starting from $h = 0$. Under such behavior, the term air entry value is referred to the soil matrix with the value of $\theta_{SM}$ being constant from $h = 0 - dh$ to $h = h_A$ where $\theta_{SM}$ denotes saturation of the soil matrix. At a very small value of $h$ (and of $\theta$ as well) we meet again the condition of $d\theta/dh \rightarrow 0$ on the MDC. The corresponding value of $\theta$ is called the residual (or minimal or intrinsic) soil water content. When it is the limit of the continuity of liquid water in soil, we denote it as $\theta_{Wr}$ (Luckner et al., 1989). When it is just a fitting parameter obtained when experimental data are fitted to an empirical equation of a SWRC, we denote it as $\theta_r$.

An analytic expression of the SWRC is advantageous for the solution of practical problems. Except for values of $\theta$ close to $\theta_S$ the SWRC resembles the hyperbola

$$|h| = a\,\theta^{-b} \tag{4.40}$$

where $a$ and $b$ are empirical constants. Because of the large variations of $\theta_S$ that occur in the field, the utility of (4.40) is increased substantially if the soil water content $\theta$ in (4.40) is replaced by the relative soil water content $\theta_R = \theta/P$ or by the relative soil water saturation $\theta_R^* = \theta/\theta_S$ (Simmons et al., 1979). An analysis based upon capillary and adsorption theories obtained by Mitchurin (1975) led to the more complex expression

$$|h| = a\,A_m\left(w - 2w_m\right)^{-b} \tag{4.41}$$

where $a$ and $b$ are physically based constants defined in a model where the soil is represented by individual particles, $A_m$ the specific surface of the particles, $w$ the mass water content and $w_m$ the mass water content when a monomolecular layer of water exists on the particles. The advantage of (4.41) is its physical interpretation of the coefficients in (4.40) that applies in the region $-\infty < h < -0.3$ MPa.

After an exhaustive study of experimentally determined SWRC on many soils, Brooks and Corey (1964) rewrote (4.40) to be

$$\theta_E = \left(\frac{h_A}{h}\right)^{\lambda} \tag{4.42}$$

where the effective water content $\theta_E = (\theta - \theta_r)/(\theta_S - \theta_r)$ and $\lambda$, the pore size distribution index, is a characteristic of the soil with values approximately equal to 2 to 5. The value of $\lambda$ is large for soils having a uniform pore size distribution and small for soils with a wide range of pore sizes.

Among the less frequently used expressions of $\theta(h)$ are hyperbolic, error function or exponential equations of other authors. For the convenience of analytic or approximate solutions of some elementary hydrologic processes, the SWRC can be formulated by still another equation which is well suited to the mathematical development of the solution (Broadbridge and White, 1988), however its practical applicability for experimental data has

not yet been proved.

Inasmuch as (4.42) does not offer a satisfactory description of the SWRC in the wet region, especially for soils not exhibiting a distinct value of $h_A$ or $h_W$, van Genuchten (1980) proposed the equation

$$\theta_E = \left[1 + \left(\alpha |h|\right)^n\right]^{-m} \tag{4.43}$$

where $\alpha$, $n$ and $m$ are fitting parameters with their limitations being $\alpha > 0$, $n > 1$, $|h| \geq 0$ and $0 < m < 1$. Values of $n$ occur between 1.2 and 4 and those of $\alpha$ between $10^{-3}$ and $10^{-2}$ $cm^{-1}$. Because of computational expediency, values $m$ have arbitrarily been taken equal to $(1 - 1/n)$. van Genuchten and Nielsen (1985) have proposed for pragmatic reasons to merely consider $\theta_r$ and $\theta_S$ as empirical fitting parameters. Note that the physically real residual water content on the SWRC in Fig. 2 was denoted by $\theta_{Wr}$. Equation (4.43) can be adopted to describe each of the branches of the hysteretic loop. The detailed procedure for expressing MDC, MWC and the scanning curves by a modified (4.43) is described by Luckner et al. (1989). Usually, $\alpha_w \approx 2\alpha_d$ where $w$ denotes wetting and $d$ is for drainage. Equation (4.43) does not allow the existence of $h_A$ and (4.42) is not suitable if an inflection point exists on the SWRC. Hence, a compromise description of the SWRC is achieved when $\theta_E$ is replaced by $\theta_e$, especially if the SWRC is further used for the determination of the unsaturated hydraulic conductivity (Šír et al., 1985). The definition of $\theta_e$ requires that $\theta$ be replaced by $\theta_e = (\theta - \theta_b)/(\theta_a - \theta_b)$, and hence, (4.43) becomes

$$\theta_e = \left[1 + \left(\alpha |h|\right)^n\right]^{-m} \tag{4.44}$$

where $\theta_a$ and $\theta_b$ are considered only as fitting parameters without physical significance and having values $\theta_a > \theta_b$ and $\theta_a \geq \theta_S$. Note however, in the range $h_A \leq h \leq 0$ that this SWRC described by (4.44) is valid only in the range $\theta_b \leq \theta \leq \theta_S$ for $\theta_b > 0$, or $0 \leq \theta \leq \theta_S$ if $\theta_b < 0$. All three equations (4.42), (4.43) and (4.44) are schematically demonstrated in Fig. 3. For large values of $\theta_a$ compared to that of $\theta_S$, (4.44) is nearly identical to (4.42).

The authors of all equations assume implicitly that $\theta_S$ is a simply measured, reliably quantified value. However, when $\theta_S$ is measured in the field, this assumption is rarely fulfilled and the resulting inaccuracy can easily destroy all the refinements of the above theoretical approaches.

In some instances, when experimental values of $\theta$ near saturation indicate the existence of a bi-modal porosity (Othmer et al., 1991), it may be more appropriate to consider that the SWRC is composed of two curves, more about it in the chapter 4. Bi-modality is evident when a smooth curve drawn through experimental data exhibits three inflection points instead of one.

## 3. Models of Soil Water Retention Curves

The simplest model of the soil porous system is a bundle of parallel capillaries, see Fig. 4. A refinement of this model considers the capillaries as being rosary (ink-bottle) tubes. Still another refinement allows hysteresis owing to the behavior of contact angles.

When the scale of the soil water pressure head on the axis of the SWRC is replaced by that of the radius of the capillaries according to (4.11), we obtain the summation curve of the pore size distribution. The derivative of this summation curve is the frequency curve of the pore size distribution. The frequency curve is advantageously expressed by equations of probability density functions (Brutsaert, 1966). Among the more common functions are the incomplete gamma distribution, the log-normal distribution and the first asymptotic

distribution. Criteria for optimal selection of the applied probability density function are the same as those used in ordinary statistics, e.g. the $\chi^2$ test or Kolgomorov-Smirnov test. A frequency curve can be used to discuss the quality of the soil pore space and the influence of society's activity upon its alteration.

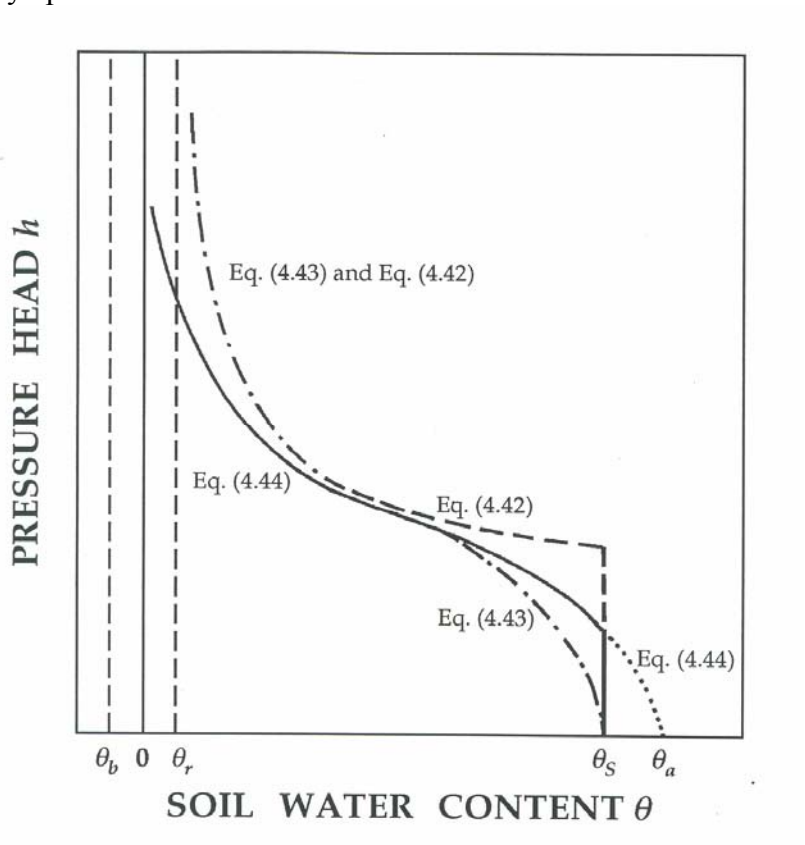


Fig. 3. SWRC represented by equations (4.42), (4.43), (4.44)

Parallel capillary tube models are distinctly different from real porous systems of soils (Dullien, 1979). Some improvement is gained when the pores formed between the contacts of soil grains are considered. Arya and Paris (1981) assumed that the similarity between the shapes of the particle-size distribution curve and the SWRC is closely related to the value of the representative pore diameter in each of the defined particle-size classes. Tyler and Wheatcraft (1989) defined an empirical coefficient $\alpha$ that relates the fractal dimension of the pore space and expresses a measure of the tortuosity of the pore space. The main disadvantage of models based upon particle-size is their negligence of the internal architecture of soil. The porous system of a soil is formed by a certain configuration of particles into aggregates and the aggregates further being arranged in a definite way. However, when the particle-size distribution of a soil is measured, the macro- and micro-aggregates are destroyed and individual particles separated.

Fatt (1956) was probably the first to realize that imperfections in parallel capillary models required a new approach to model porous media. He proposed an empirical, two-dimensional network of capillaries having randomly distributed radii. This lattice type network of pores was extended to a 3-dimensional network and for the solution of equilibria between the soil water potential and $\theta$, percolation theory was applied (Chatzis and Dullien, 1977; Wardlaw et al., 1987; and Diaz et al., 1987). With the soil water potential being

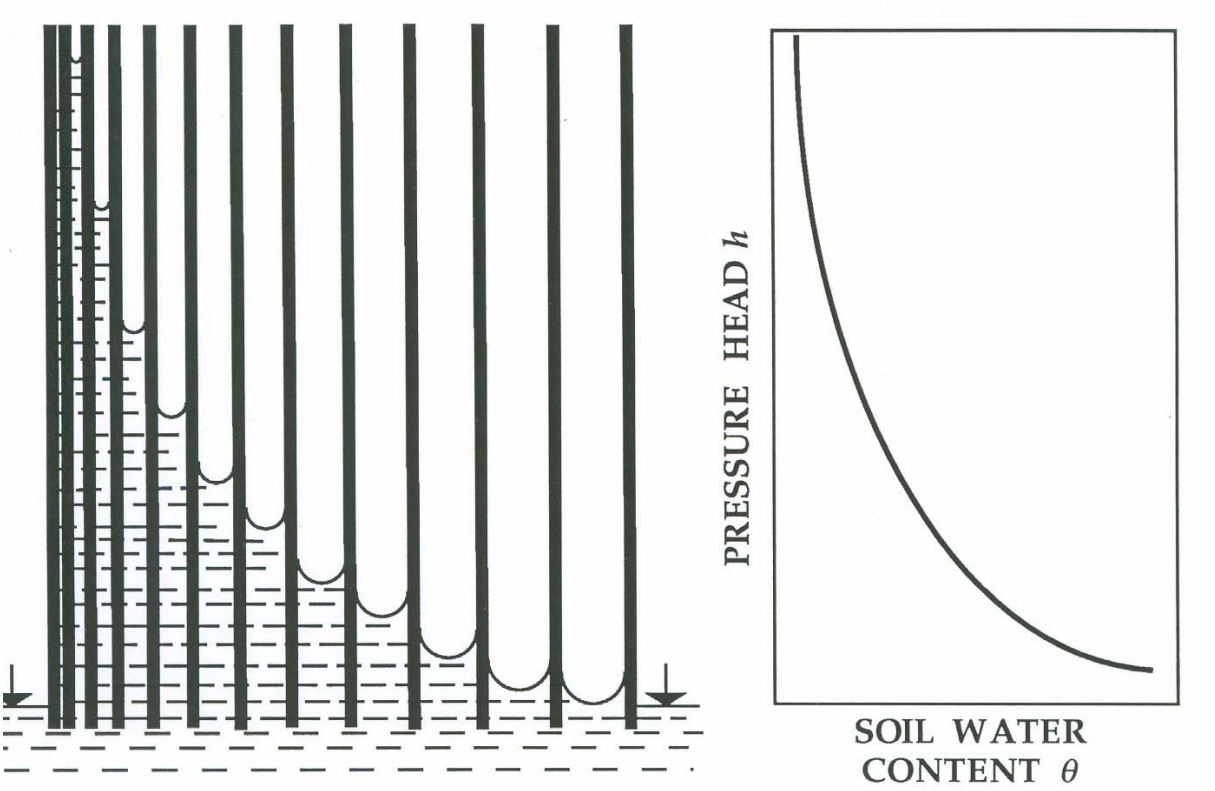


Fig. 5. The simplest model of SWRC consisting of parallel capilary tubes (left) and the resulting SWRC (right)

identified with the capillary potential, the model was hypothetically placed into the pressure apparatus. We shall first use the simplest type of percolation model which is a 2-dimensional square network where the pores are represented by mutually interconnected perpendicular cylindrical tubes of various radii. The radii are scattered randomly in the network with a prescribed distribution function $\rho(r)$. Inasmuch as the number of segments $n$ approaches infinity in percolation theory, models of the theory usually contain segments $n > 1000$. Here for the sake of clarity in Fig. 6, we use only 72 segments.

This 2-dimensional model is conceptually first completely saturated with water and placed in a pressure plate apparatus. Similar to the method described in section 4.3.1, the air pressure is gradually and incrementally increased. When the pressure head $h$ is below the percolation threshold $|h| < h_p$ , water is replaced only in a very small portion of pores of radii $r$ defined by (4.11) as

$$r \geq r_h = \frac{2\,\sigma \cos\gamma}{|h|\,\rho_W\, g}. \qquad (4.45)$$

The great majority of pores having radii $r \geq r_h$ is surrounded by pores having radii of $r < r_h$. At this small initial value of pressure head $h$, the cluster of air-filled pores close to the top surface of the model is negligible and the model is not effectively drained. When the air pressure in the apparatus reaches the percolation threshold $h_p$, water is replaced by air in a continuous cluster of pores, all of radii $r \geq r_{hp}$, see Fig. 6. Isolated groups of water-filled connections of radii $r > r_{hp}$ remain undrained because they are surrounded by air-filled connections leaving them isolated and without a continuous path to the semipermeable membrane of the apparatus and to the free water pool. When the air pressure is further increased in our model, no additional drainage is realized and this is denoted as the post-percolation stage. A SWRC of such a model is step-like.

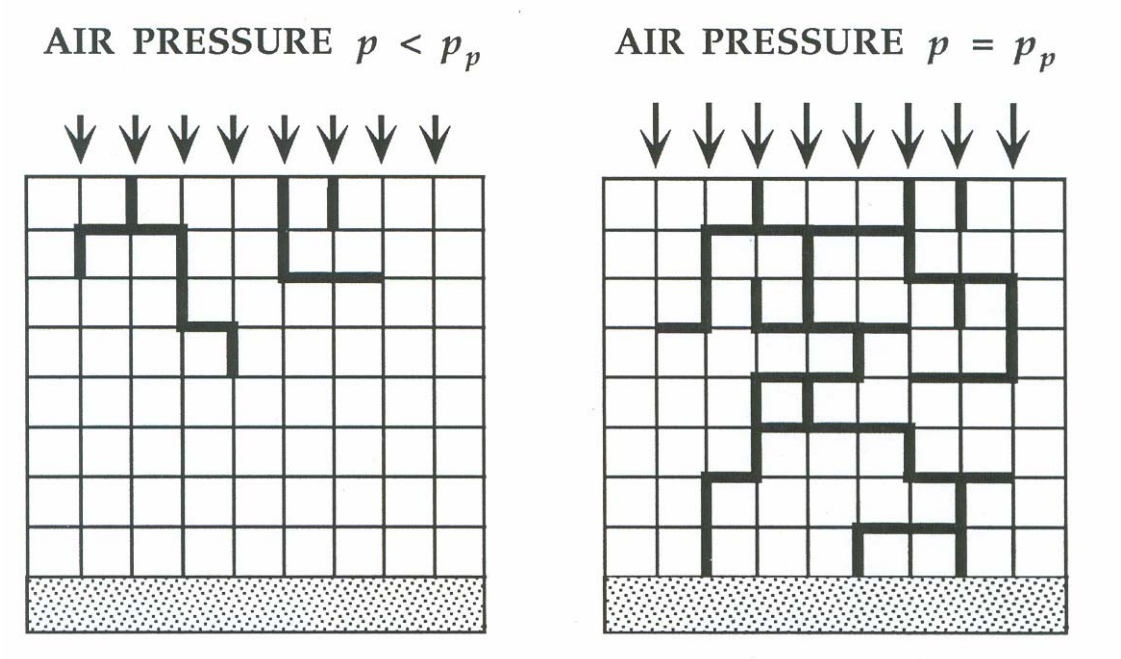


Fig. 6 Pre-percolation (left) and percolation stage (right) in a 2-dimensional model consisting of capillary tubes of randomly distributed radii. Thick lines denote capillary tubes filled with air when the model is placed into a pressure apparatus.

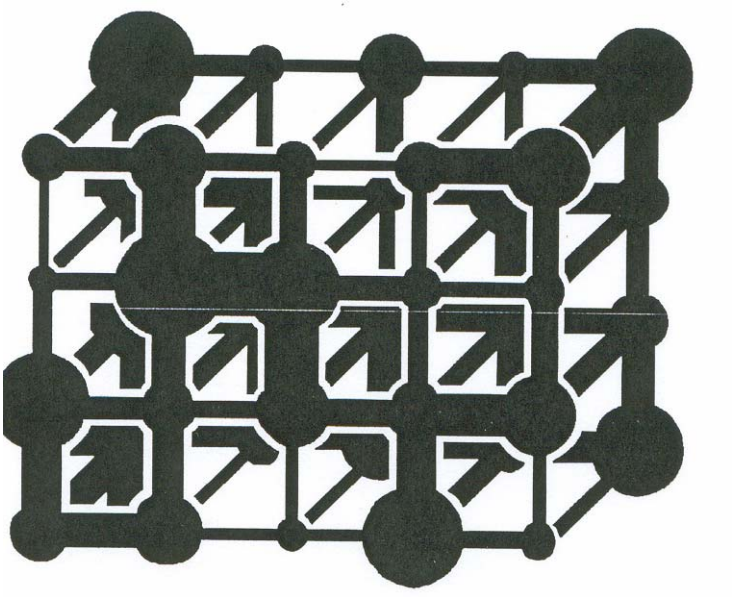

Fig. 7. A 3-dimensional model consisting of spherical pores interconnected by capillary tubes (throats) whose radii are randomly distributed. The model functions in principal analogically to model in Fig. 6 with pre-percolation and percolation stages.

When the model still consisting of perpendicular capillary tubes is extended to a 3-dimensional net, drainage does not stop at one percolation stage but proceeds further when the

external pressure is increased. The SWRC of the 3-dimensional net does not yield a unique step-like form similar to that of the 2-dimensional model. Owing to the three dimensionality of the net, clusters of undrained pores change and alter their configuration with a portion of undrained water remaining. Similarly, when water enters into a dry, air-filled model, clusters of pores remain filled with air in spite of the fact that they should be filled with water at the given pressure if water had free access to all pores. This procedure adequately explains the mechanistic part of hysteresis. With the occurrence of the clustering of entrapped water or air, the restrictive access of pore water or pore air to the outside pool of free water or free air is demonstrated.

Another type of 3-dimensional model consists of spherical pores interconnected by capillary tubes (throats). They are arranged in a cubical net, see Fig. 7. The throats may or may not be correlated to the spherical pores. With radii of pores randomly distributed, the distribution function and skewness are described. An increase of the standard deviation increases the slope of the SWRC. Or, $\alpha$ and to a lesser extent $n$ in (4.43) decrease their numerical values. The air entry value depends upon the skewness of this distribution curve (Rösslerová, 1993). The model can be expanded to a bi-modal porosity with hierarchical arrangement of sub models (peds) within the cubic net (Kutílek et al., 1992). This type of

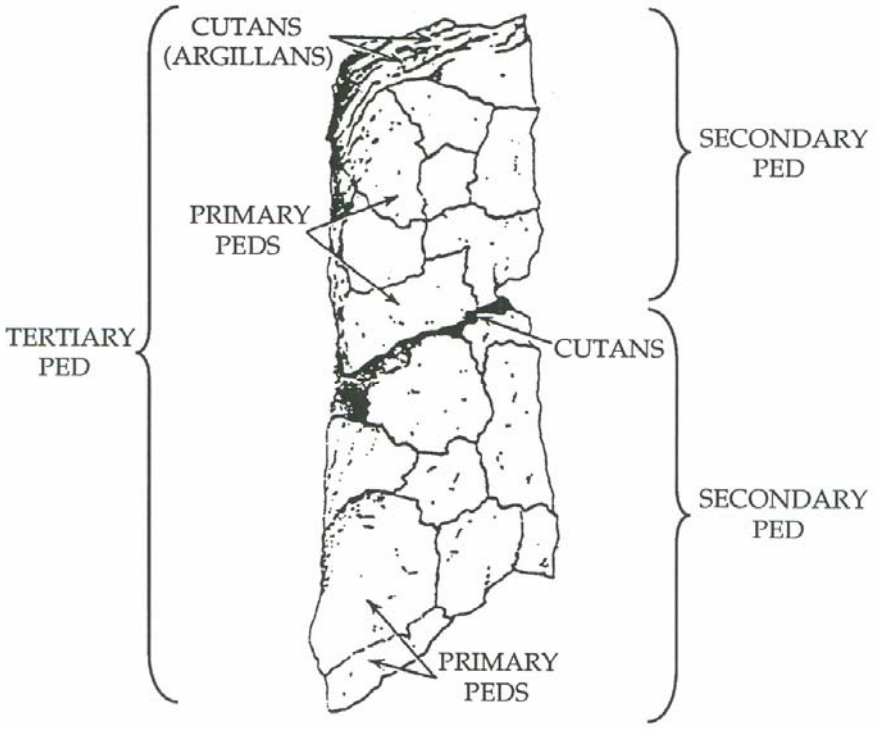


Fig. 8.The soil fabric manifests primary peds formed by solid constituents arranged into secondary and tertiary peds.

model corresponds nicely with the porous system found in the crumb structure of the A horizon of a soil. Numerical studies of this hierarchical arrangement confirm the existence of three inflection points on the SWRC. As it follows from studies of Rösslerová (1993), SWRC are more realistic to natural soils if bimodality is introduced. The slope of the SWRC is increased and the values of parameters $\alpha$ and $n$ in (4.43) decrease owing to bimodality, especially for soils consisting of large peds. Moreover, the value of $\theta_r$ increases in such soils compared with that of monomodal soils. Bimodal soil systems manifest a broader hysteretic

loop and generally, the amount of water or air residing in enclosed clusters is increased during the entire drainage or wetting process.

The configuration of pores between peds may be different from that within the matrix. In B horizons we frequently observe polyhedral or cubic structure which is modeled by cubes. The pores between the peds correspond approximately to a system of perpendicular slits having widths that are randomly distributed and defined by a prescribed distribution function.

The hierarchical arrangement of pores can proceed beyond the bimodal concept if we find primary, secondary and tertiary peds in a soil horizon, see Fig. 8. Generally, models of soil porous systems should properly mimic the morphological reality of the soil and the classification used in soil macro- and micro morphology (U. S. Soil Taxonomy, 1975; Brewer, 1976; and Jim, 1988).

Further progress in conceptually modeling of soil porous systems is achieved by the application of fractal geometry, especially when the soil is fragmented owing to aggregation. The self-similarity in porous systems of secondary and tertiary peds in Fig. 8 is distinct. Rieu and Sposito (1991) have discussed various types of models of fractal porous media with regard to real soils. Apparently, two avenues for model characteristics from soil analysis are available. Using aggregate size distribution data, Rieu and Sposito's (1991) simulated SWRC of an aggregated silty loam was close to measured data. Another avenue is the image analysis of micro- and macro-morphological studies usually presented as photos of either thin sections or of a topography of a plane. In both cases, the pores are distinctly identified. Macromorphological fractal analysis of staining patterns of macropores presented by Hatano and Boolting (1992) yielded fractal dimensions related to by-pass flow.

The above-mentioned refinement of models and procedures contribute to a more realistic conceptualization of the mechanical components of the total soil water potential in the wet portion of the SWRC. For the dry portion of the SWRC those improvements are practically irrelevant. Hence, we should concentrate on the force field at the molecular scale provided that we really need to interpret the dry part of the SWRC for a more accurate formulation of the processes.

Inasmuch as the surface tension of water $\sigma$ depends upon the temperature, we expect the SWRC to be effected by temperature. A temperature increase induces a decrease in the value of $\sigma$, and consequently the capillary height decreases. Accordingly, for a given soil water content, the value of the pressure head $h$ increases (i.e. $|h|$ decreases). However, Novák (1975) and Hopmans and Dane (1986) report that the changes of the SWRC are greater than those expected just from $\sigma(T)$. Apparently, differences between theoretical and experimental values of $h(\theta, T)$ cannot be explained solely upon the basis of entrapped air as earlier assumed. A final conclusion based upon many experiments is that capillarity alone is not sufficient to explain water retention in soils even in the "wet" part of the SWRC. Therefore, all pore size distribution functions remain approximate if they are only based on capillary models.

# 4. SWRC INTERPRETED AS PORE SIZE DISTRIBUTION MODEL

In spite of the early studies of the various types of distribution functions of soil pores by Brutsaert (1966), it lasted for 25 years, until the log-normal pore-size distribution was applied to the form of the retention curve $h(\theta)$ (Pachepsky et al., 1992, Kosugi 1994), and to $K(\theta)$ (Kosugi, 1999). In all quoted studies, the distribution function was obtained as the derivative curve.

Even if the distribution function on a log-normal scale may be more or less skewed, its log-normal form seems to be a useful approximation, at least as for the time being. The retention curve and the derived conductivity function based on the pore size distribution have the advantage of the physical interpretation of the SPS, even if still in an approximate way.

The log-normal pore radius distribution function $g(r) = \mathrm{d}\theta/\mathrm{d}r$ is (Pachepsky et al., 1992, Kosugi, 1994)

$$g(r) = \frac{\theta_S - \theta_R}{\sigma r\sqrt{2\pi}} \exp\left\{ - \frac{[\ln(r / r_m)]^2}{2\sigma^2} \right\} \tag{4.46}$$

where $r$ is the pore radius, $r_m$ is the geometric mean radius, $\sigma$ is the standard deviation. The soil water retention curve as a cumulative curve is

$$S = \frac{1}{2} erfc\left[ \frac{\ln(h / h_m)}{\sigma \sqrt{2}} \right] \tag{4.47}$$

where $S$ is defined by Eq. (4.48), $erfc$ is the complementary error function, $\ln h_m$ is the mean of the log-normal distribution $f(\ln h)$

$$S = \frac{\theta - \theta_R}{\theta_S - \theta_R} \tag{4.48}$$

$\theta_R$ is the residual soil water content when the liquid flow is essentially zero. The value of $\theta_R$ is usually not measured but it is found as a fitting parameter, and $\theta_S$ is the soil water content at saturation.

The detailed study of $h(\theta)$ of the porous system of majority of soils led to the discovery of bi- and multi-modal porosity (Othmer et al., 1991, Durner, 1992, Pachepsky et al., 1992) due to the structural characteristics of soils. The phenomenon will be demonstrated on the soil denoted as SO15, see Fig.1. The soil is a well structured A horizon of Hapludalf. First, the SWRC $\theta(h)$ is transformed to parametrized form $S(h)$ and its derivative curve is computed and plotted:

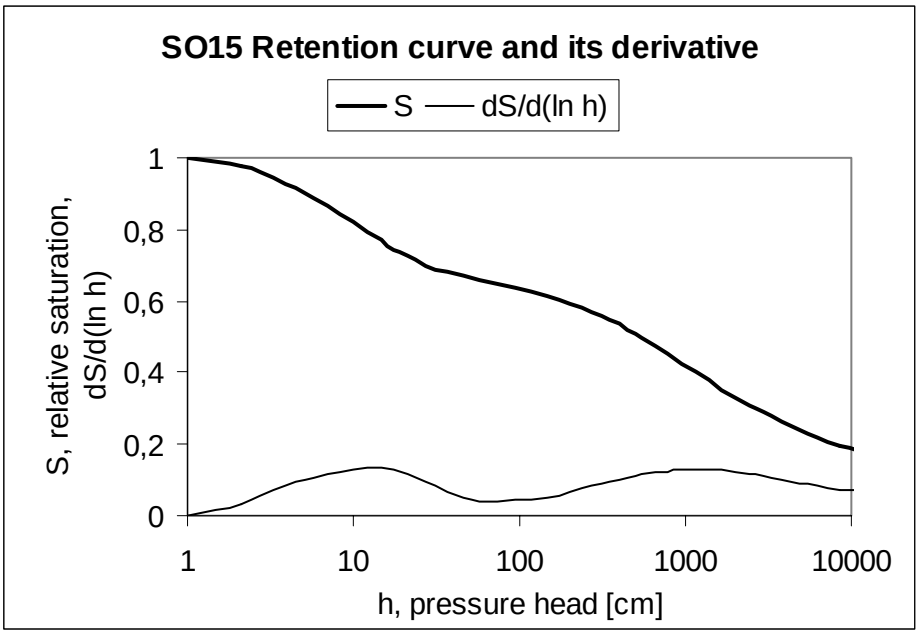


Fig. 9. The retention curve in Fig. 1 was transformed to $S(h)$ and its derivative curve was plotted. It represents the pore size distribution in the bi-modal soil. The structural domain (left side) is separated from the matrix domain (right side) by $h_A$ = 60 cm at the minimum of the derivative curve.

If the pressure head is related to the pore radius by $r$ (μm) = 1500/$h$ (cm), we obtain a real pore size distribution, see Fig. 10.

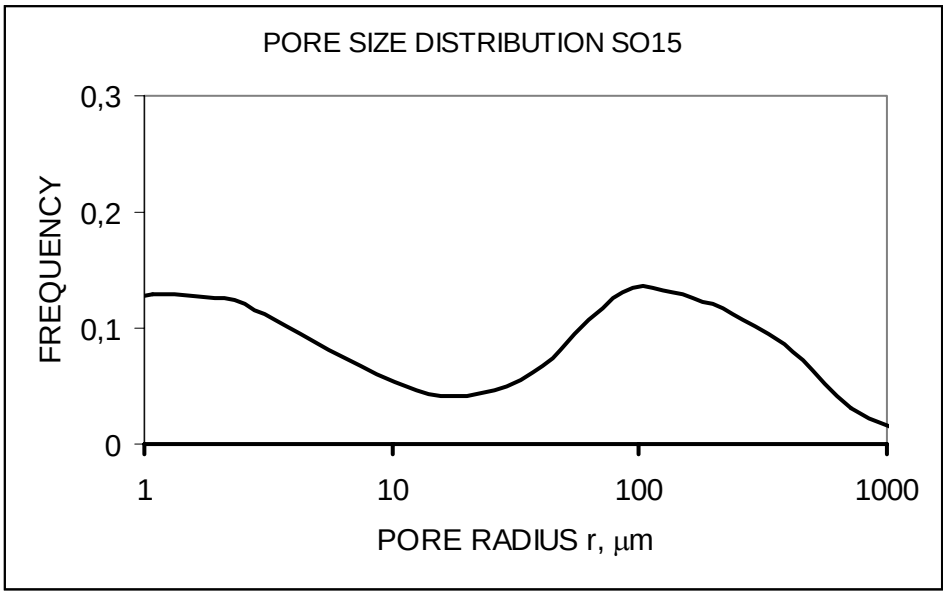


Fig. 10 Pore size distribution derived form the derivative curve in Fig. 9. The separation of structural from the matrix domain is at $r_A$ = 25 μm, structural domain is at 1000> $r$ > 25 μm, matrix domain is at $r$ < 25 μm.

The curve shows two peaks of separated domains in majority of instances in structured soils, one peak of matrix pores (denoted by index 1) and another one of structural pores (indexed by 2). When we separate those two domains, we obtain two log-normal pore radius

distribution functions with $i = 1$ for matrix and $i = 2$ for structural pores and for each domain equations (4.46), (4.47) and (4.48) are modified.

$$g_i(r) = \frac{\theta_{Si} - \theta_{Ri}}{\sigma_i r\sqrt{2\pi}} \exp\left\{ - \frac{[\ln(r / r_{mi})]^2}{2\sigma_i{}^2} \right\} \tag{4.49}$$

and two soil water retention curves

$$S_i = \frac{1}{2} erfc\left[ \frac{\ln(h_i / h_{mi})}{\sigma_i \sqrt{2}} \right] \tag{4.50}$$

where

$$S_i = \frac{\theta_i - \theta_{Ri}}{\theta_{Si} - \theta_{Ri}} \tag{4.51}$$

where $i = 1$ is for matrix pores and $i = 2$ for structural pores. With the principle of superposition, applied already by Othmer *et al.* (1991), Pachepsky *et al.* (1992) and by Zeiliguer (1992) we define for bi-modal soils

$$\theta = \theta_1 + \theta_2 \tag{4.52}$$

Since coarse micropores of $r > r(h_A)$ would cause instability of aggregates, we assume that the matrix porous system does not contain coarse micropores above $r(h_A)$. Then

$$\theta_{S1} = \theta(h_A) \tag{4.53}$$

and

$$\theta_{S2} = \theta_{S\,(MEAS)} - \theta_{S1}. \tag{4.54}$$

where $\theta_{S\,(MEAS)}$ denotes the measured saturated water content.
For $0 > h \geq h_A$ is

$$\theta_1 = \theta_{S1}, \quad S_1 = 1 = \text{const.} \tag{4.55}$$

$$\theta_2 < \theta_{S2}, \quad S_2 < 1 \tag{4.56}$$

For $h < h_A$ is

$$\theta_1 < \theta_{S1}, \ S_1 < 1 \tag{4.57}$$

We assume that $\theta_{R1}$ in $S_1$ is physically below the wilting point $\theta_{WP}$ ($h$ = -15000cm) in the range of hygroscopic water and we approximate $\theta_{R1} = 0.5\ \theta_{WP}$. For structural domain we take $\theta_{R2} = 0$.

The evaluation of SWRC of pores in structural and in matrix domains is in Fig. 11.

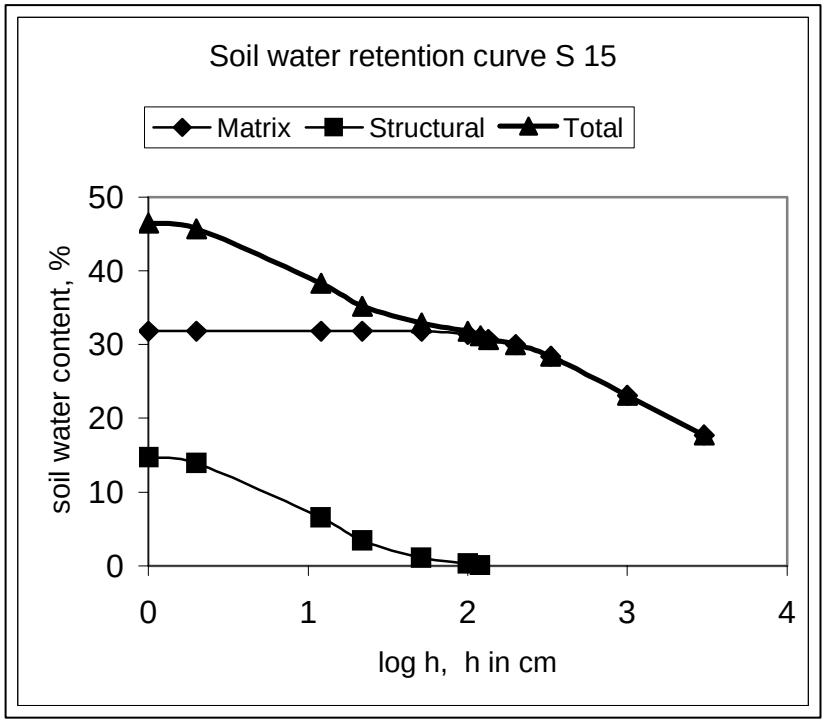


Fig. 11. Separation of soil water retention curves into SWR of matrix and SWRC of structural domains in SO15 soil.